Influence of molecular reorientation on electronic energy transfer between a pair of mobile chromophores: The stochastic Liouville equation combined with Brownian dynamic simulation techniques

Igor Fedchenia and Per-Olof Westlund*
Department of Physical Chemistry, University of Umeå, S-901 87 Umeå, Sweden
(Received 21 September 1993; revised manuscript received 15 December 1993)

An algorithm is developed in order to solve the stochastic Liouville equation describing energy transfer between a donor-donor pair of reorienting chromophores. The algorithm requires the fluctuating part of the Liouville equation in the form of trajectories. In this particular case the molecular reorientation of the chromophores was simulated by means of a Brownian dynamic simulation technique where each of the two molecules are allowed to undergo a restricted rotational diffusion in a cone potential. Numerical results are presented for the correlation function $\langle \chi(t)\chi(0)\rangle$, representing the probability that the initially excited donor still is excited at a later time t. Results are given for the weak or Förster regime and for a simple case in the strong or slow motion regime. The time resolved fluorescence anisotropy $r(t)$ is also calculated for different molecular reorientational rates and cone potentials.

PACS number(s): 87.15.−v

I. INTRODUCTION

An electronically excited molecule may be relaxed due to energy transfer to another molecule. For large separation this transfer is dominated by a dipole-dipole interaction between the two molecules. This energy transfer mechanism is used extensively for interpretation of photophysical studies of molecular systems active in photosynthesis. The Förster theory [1] describes energy transfer or radiationless transport of excitons between pairs of immobile molecules (donors and acceptors) by virtue of intermolecular electron transition dipole-dipole interaction. Förster showed that the electronic energy transfer rate constant for weakly coupled pairs of chromophores is given by $W(r,\Omega)$,

$$W(r,\Omega)=\frac{1}{\tau}\frac{3}{2}\kappa^2(\Omega)\left[\frac{R_0}{r}\right]^6, \quad (1)$$

and thus is proportional to the inverse sixth power of the intermolecular distance r between the pair of fluorescent molecules. The square of the orientation function is κ, the lifetime of the excitation is τ, and R_0 is the so-called Förster radius [1]. The dependence on orientations of the two transition moments relative to the vector $\mathbf{r}$ joining the two molecules is given by

$$\kappa(\theta_A,\theta_D,\phi_{AD})=2\cos\theta_A\cos\theta_D-\cos\phi_{AD}\sin\theta_A\sin\theta_D$$
$$=\boldsymbol{\mu}_A\cdot\boldsymbol{\mu}_D-3(\boldsymbol{\mu}_A\cdot\mathbf{r}_{AB})(\boldsymbol{\mu}_D\cdot\mathbf{r}_{AD}), \quad (2)$$

with $\phi_{AD}=(\phi_A-\phi_D)$. Here, $\boldsymbol{\mu}_\gamma$ represent a molecular fixed unit vector along the transition dipole of molecule γ.

The angle dependence in $\kappa(\Omega)$ becomes a random function in time as a consequence of reorientation of the two chromophores. Förster's expressions presuppose that only dipole-dipole coupling is active between the molecules and that dynamics effects due to molecular reorientation are absent. The effects of molecular dynamics may be included in the description of energy transfer through the basic stochastic Liouville equation (SLE) [2]. The SLE formalism then treats the energy transfer process within the same conceptual framework as other relaxation processes. Within a simple two-site dynamic model, equations were derived including the effect of molecular reorientation and analogous to the master equation of Föster's theory [2]. Förster's master equation was derived from the stochastic Liouville equation by a simple perturbation treatment determining precisely under what conditions the master equation can be used [2].

A theoretical framework for treating energy transfer between pairs of chromophores undergoing free or restricted molecular motion on the same time scale as the energy transfer process has not yet been given in the literature. We believe that the SLE approach combined with Brownian dynamic simulation (BD) presented in this work is a very useful approach and sufficiently flexible to meet the problem of describing energy transfer between pairs of chromophores attached to proteins or other macromolecules. An alternative approach to the STE approach is to use the kinetic master equation where molecular dynamics effects may be included by introducing explicit trajectories of Brownian dynamic simulation into $\kappa^2(\Omega)$ of the Förster transition rate constant [3].

The system of interest in this work is schematically shown in Fig. 1 and consists of a pair of chromophores, for instance, that are covalent bound at fixed intermolecular distance r_{AD} in a protein or some other macromolecule. The chromophore pair may be incorporated at different distances r_{AD}, thus making it possible to tune

*Author to whom correspondence should be addressed.

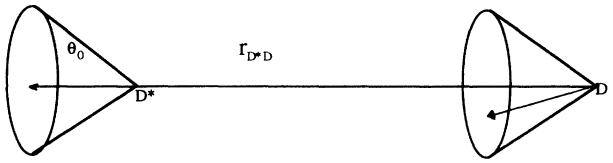

FIG. 1. A schematic representation of the geometrical configuration of a donor-donor pair of chromphores with one excited donor (D^*). The donors are reorienting independently from each other within a cone potential defined by the semiangle θ_0.

the coupling strength and accordingly the rate of the energy transfer mechanism. In this work we present numerical results for cases where the dipole-dipole coupling strength has been varied from "strong" to the weak perturbation regime, with "strong" coupling or the "slow-motion" regime using the usage from electron spin resonance (ESR) and paramagnetic nuclear spin relaxation theory. The slow-motion regime is defined by the relation $HDD\tau_{DD} \geq 1$ where H^{DD} is the interaction strength and τ_{DD} the characteristic correlation time of the fluctuating dipole-dipole coupling.

Chromophore molecules that are covalent bound to a macromolecule are expected to reorient in a restrictive way. In this work we have modeled the chromophore reorientational dynamics as a restricted Brownan diffusion motion in a cone potential (wobbling in a cone). The cone potential V_{con} is defined by the semiangle θ_0,

$$V_{\text{con}} = \begin{cases} 0 & \text{for } 0 \leq \theta < \theta_0 \\ \infty & \text{for } \theta = \theta_0 \end{cases} . \tag{3}$$

The outline of this paper is as follows: In Sec. II the SLE approach is reviewed. The stochastic fluctuation of the dipole-dipole coupling is determined explicitly by the Brownian dynamic simulation technique. In Sec. III the numerical approach is presented and a new algorithm developed that solves the stochastic Liouville equation effectively. We apply the SLE to energy transfer when the two molecules are allowed to rotate in identical cone potentials. In Sec. IV numerical results are presented for the correlation function describing the probability that the initially excited chromophore sill is excited at a later time t. We discuss both the weak perturbation limit and the strong coupled regime where oscillations of the excitation between the chromophores are pronounced. The fluorescence anisotropy is also calculated for different dynamics cases. Finally, we summarize the main results of this paper.

II. ENERGY TRANSFER BETWEEN A PAIR OF DIPOLE-DIPOLE COUPLED MOLECULES

A. The stochastic Liouville equation of motion

The equation of motion for the electron density operator, describing energy transfer between two dipole-dipole coupled chromophores, was given by Agranovich and Galanin [4] for an immobile pair. In the superoperator formalism the stochastic Liouville equation of motion was used in [2]. The state of the combined system is described as a direct product $\rho_A \otimes \rho_D$ of two electron density operators ρ_A and ρ_D. The Liouville formalism is used for the energy transfer between two molecules, an excited donor D and a ground-state acceptor A. For each molecule we assume that the first excited state $|1\rangle$ and the ground state $|0\rangle$ are relevant for the problem. The time evolution of the density matrix follows from the Liouville equation of motion:

$$\frac{\partial}{\partial t}\rho_A \otimes \rho_D = -i\{L_A + L_D + L_{AD}(t)\}\rho_A \otimes \rho_D , \tag{4}$$

where the Liouville superoperators L_A and L_D specify the isolated chromophores and L_{AD} is the Liouville superoperator generated by the intermolecular dipole-dipole interaction $H^{dd}(t)$ [3]. The coupling L_{AD} originates from the dipole-dipole interaction whose Hamiltonian H^{DD} is given by

$$H^{DD} = \frac{\mu_A \mu_D 1}{4\pi\varepsilon_0 r_{AD}^3}\kappa(\Omega) , \tag{5}$$

where $\kappa(\Omega)$ is defined in Eq. (2) and μ_A and μ_D are the transition dipole operators, r_{AD} the distance between the donor and the acceptor, and ε_0 the permittivity of vacuum. The Liouville operator L_{AD} is obtained from H^{DD} as a derivation superoperator [5]. For the special case of fixed intermolecular distance r_{AD} the stochastic fluctuating factor $\kappa(\Omega)(t)$ is due to internal rotation diffusion of the two chromophores. No local field approximations have been introduced in Eq. (5). For real systems one may introduce the refractive index to consider local effects but still assume that the only reorientation dependence is in $\kappa(\Omega)(t)$.

The density matrices ρ_A and ρ_D have only four matrix elements, respectively. We express them in terms of the basis operators

$$\begin{aligned} &\rho_1^j = |0\rangle\langle 0| , \quad \rho_2^j = |1\rangle\langle 1| , \\ &\rho_3^j = |0\rangle\langle 1| , \quad \rho_4^j = |1\rangle\langle 0| , \end{aligned} \tag{6}$$

where $j = A$ or D and $|1\rangle$ and $|0\rangle$ denote the excited and ground states, respectively. We may transform to a set of (left) eigenoperators representing the equilibrium state $(\rho_1 = |0\rangle\langle 0| + |1\rangle\langle 1|)$ and the nonequilibrium state $(\rho_1 = |1\rangle\langle 1|)$ under the assumption that $\omega_j = E_{1,j} - E_{0,j} \gg kT$. We now have four eigenoperators of the electronic part of the Liouville iL_j, with eigenvalues (in angular frequency units)

$$\begin{aligned} &\lambda_1 = 0 , \quad \lambda_2 = \tau_j^{-1} , \\ &\lambda_3 = -i\omega_j - \frac{1}{T_{2,j}} , \quad \lambda_4 = i\omega_j - \frac{1}{T_{2,j}} , \end{aligned} \tag{7}$$

where τ_j is the lifetime of the excited state of molecule j without energy transfer, $\omega_j = E_{1,j} - E_{0,j}$. $1/T_{2j}$ is the width of the assumed Lorentzian absorption peak at the resonance frequency ω_j.

The primary observable is the time evolution of the combined state of an initially excited donor and a nonexcited acceptor state. In terms of the density operators it

refers to the time evolution of $[\rho_1^A\rho_2^D](t)$ given that the initial condition is $[\rho_1^A\rho_2^D](0)=1$; the other density matrix elements are equal to zero.

We assume that the coupling L_{AD} is weak relative to the excitation energy. The relevant states are then

$$\chi_1\equiv\rho_1^A\rho_2^D\ ,\ \chi_2\equiv\rho_2^A\rho_1^D\ ,\ \chi_3\equiv\rho_3^A\rho_4^D\ ,\ \chi_4\equiv\rho_4^A\rho_3^D\ , \tag{8}$$

since the total excited state $\rho_2^A\rho_2^D$ and the total ground state $\rho_1^A\rho_1^D$ do not couple to χ_1 to second order in L_{AD}. Out of the original 16×16 Liouville L matrix, we have now isolated a 4×4 submatrix [2,4] that contains the physically interesting couplings. The stochastic Liouville equation of motion in matrix form reads

$$\frac{d}{dt}\chi(t)=-i\mathbf{L}(t)\chi(t)\ , \tag{9}$$

where χ is the density vector of the four elements in Eq. (8). Since the stochastic Liouville matrix is written in the eigenoperators of the separate electronic systems, it has only the coupling off-diagonal and the combined eigenvalues of two electronic systems on the diagonal:

$$\mathbf{L}=\begin{bmatrix} A & 0 & H & -H \\ 0 & B & -H & H \\ H & -H & iC & 0 \\ -H & H & 0 & iC^* \end{bmatrix}\ ,$$

$$A=-1/\tau_A\ ,\ B=-1/\tau_D\ , \tag{10}$$

$$C=-1/T_{AD}-i\delta\ ,\ H=\frac{i}{\sqrt{2}}F\kappa\ ,$$

where the off-diagonal term H is given in Eq. (5) with $F=\mu_A\mu_D/[4\pi\varepsilon_0 r^3]$. The stochastic time dependence is due to the random function $\kappa(\Omega)$. C includes the overlap $1/T_{AD}=1/T_A-1/T_D$. In the strong coupled limit we cannot simply define a vibrational state independent "Förster radius" since the coupling between different vibrational states of the chromophore pair is dependent on the initial and final vibrational level. Equation 10 needs to be generalized to include vibrational transitions and their vibrational relaxation rates. In this work we leave this problem and focus on how to treat the dynamics of the Liouville matrix in Eq. (10).

Two physically interesting correlation functions are $\langle\chi_1(t)|\chi_1(t_0)\rangle$ and $\langle\chi_2(t)|\chi_1(t_0)\rangle$, representing an ensemble average of the probability that the initial excited chromophore is excited at time $t-t_0$ and the probability that the chromophore intitially not excited has the excitation at time $t-t_0$, respectively. In the numerical calculations we confine ourselves to one of the energy transfer paths where the acceptor is the same species as the donor (donor-donor); we then have $\tau_A=\tau_D$ and $\delta=0$ by symmetry.

B. The model of molecular reorientation

We explicitly incorporate the molecular reorientation processes into the SLE. In this work we have used the cone model in order to describe the molecular reorientation of the two chromphores. More specifically, the electronic transition moment of each chromophore is described by two Euler angles (θ,ϕ) $(i=A,B)$ restricted by the cone potential given in Eq. (3).

The dynamics of a chromophore is described by the diffusion equation

$$\frac{1}{D}\frac{\partial}{\partial t}P(\theta,\phi,t)=\Delta_\Omega P(\theta,\phi,t)\ ,$$
$$\Delta_\Omega=\frac{1}{\sin\theta}\frac{\partial}{\partial\theta}\left[\sin\theta\frac{\partial}{\partial\theta}\right]+\frac{1}{\sin^2\theta}\frac{\partial^2}{\partial\phi^2}\ . \tag{11}$$

The cone potential $V_{\rm con}$ leads to the boundary condition

$$\left.\frac{\partial}{\partial\theta}P(\theta,\phi,t)\right|_{\theta=\theta_0}=0\ . \tag{12}$$

As an initial condition, we took P uniform over the angular space $0<\theta<\theta_0$ and $0<\phi<2\pi$:

$$P_{\rm eq}=\left[\int_0^{2\pi}\int_0^{\theta_0}\sin(\theta)d\theta\,d\phi\right]^{-1}\ . \tag{13}$$

The model of the chromophores is characterized by the lifetime of the excitation, τ_D, the line broadening overlap T_{AD}, the transition dipole moments μ_D, and the distance between the chromophores r_{DA}. The molecular reorientational dynamic restricted in the cones for each chromophores is characterized by the diffusion coefficient D (the same for both chromphores) and the semiangle θ_0, describing the cone potential. We explicitly incorporate the molecular reorientational processes into the SLE simulating the energy transfer [cf. Eq. (9)] for different dynamics and coupling strengths.

III. NUMERICAL APPROACH

A. The stochastic time dependence of $\kappa(\Omega)$

In order to solve Eq. (9) with a stochastic time-dependent Liouville matrix, the random off-diagonal elements H must be available in the form of explicit trajectories. The algorithm described in Sec. III C is quite general and independent of the method used to generate the fluctuation terms in the stochastic Liouville equation. In our case we have used Brownin dynamic simulation techniques and the model of force-free diffusion in a cone which, as has been shown, is very useful in many different model calculations of restricted molecular diffusion, for instance, of small sections of a protein or the local dynamics of a segment of an amphiphile alkyl tail in liquid crystalline lamellar phases. In a recent work [6] we developed and tested three different algorithms to simulate restricted diffusion in a cone. Instead of using the Langevin equations for the Euler angles which have a singularity due to $1/\sin^2\theta$ of the angular part of the Laplacian operator (11) and in the corresponding Langevin equations, we used the Langevin equations in Cartesian coordinates and the algorithm presented in detail in Appendix A. In order to obtain the stochastic time dependence of $\kappa(\Omega)$, we simulate two independent trajectories moving inside a cone defined by a semiangle θ_0.

B. The statistical characteristics of the fluctuating dipole-dipole coupling (κ)

The uniform initial condition (13) and Markovian nature of the diffusion process of Eq. (11) make the random process $\kappa(\theta_A\theta_D\phi_{AD})$ stationary. The time-independent probability distribution function $P(\theta,\phi)$ is shown in Figs. 2(a) and 2(b) as a function of different semiangles θ_0 of the cone potential. $P(\theta,\phi)$ is substantially non-Gaussian and displays a very strong angle dependence. For the isotropic case ($\theta_0=180°$) we see that here are equally large amounts of configuration of the two transition dipole moment vectors giving the value of κ between -2 and 2. However, when we introduce restriction in the angular space of each cone, the distribution function loses the symmetry around $\kappa=0$. For instance, when the transition dipoles are restricted to move in the same hemisphere ($\theta_0=90$), the asymmetry becomes pronounced and positive values become more probable with a peak for approximately $\kappa=1$. As we impose larger and larger restrictions [cf. Fig. 2(b)] of the cones, which means a smaller and smaller semiangle, the peak value of the distribution function $P(\kappa)$ moves towards the value of κ corresponding to the configuration of Fig. 1 ($\kappa=2$). In Fig. 3(c) the first and second moments of κ and $\sqrt{\kappa^2}$ are displayed as a function of cone semiangle.

Since the dependence on D in Eq. (14) is a simple scaling of time, we can plot correlation function $K_1(\tau)=\langle\kappa(0)\kappa(\tau)\rangle$ as a function of $\tau=Dt$. (The Euler angles are omitted in κ for brevity.) The correlation function $K_1(\tau)$ is shown in Fig. 3(a) for three semiangles (171°, 99°, and 45°). The plateau value strongly depends

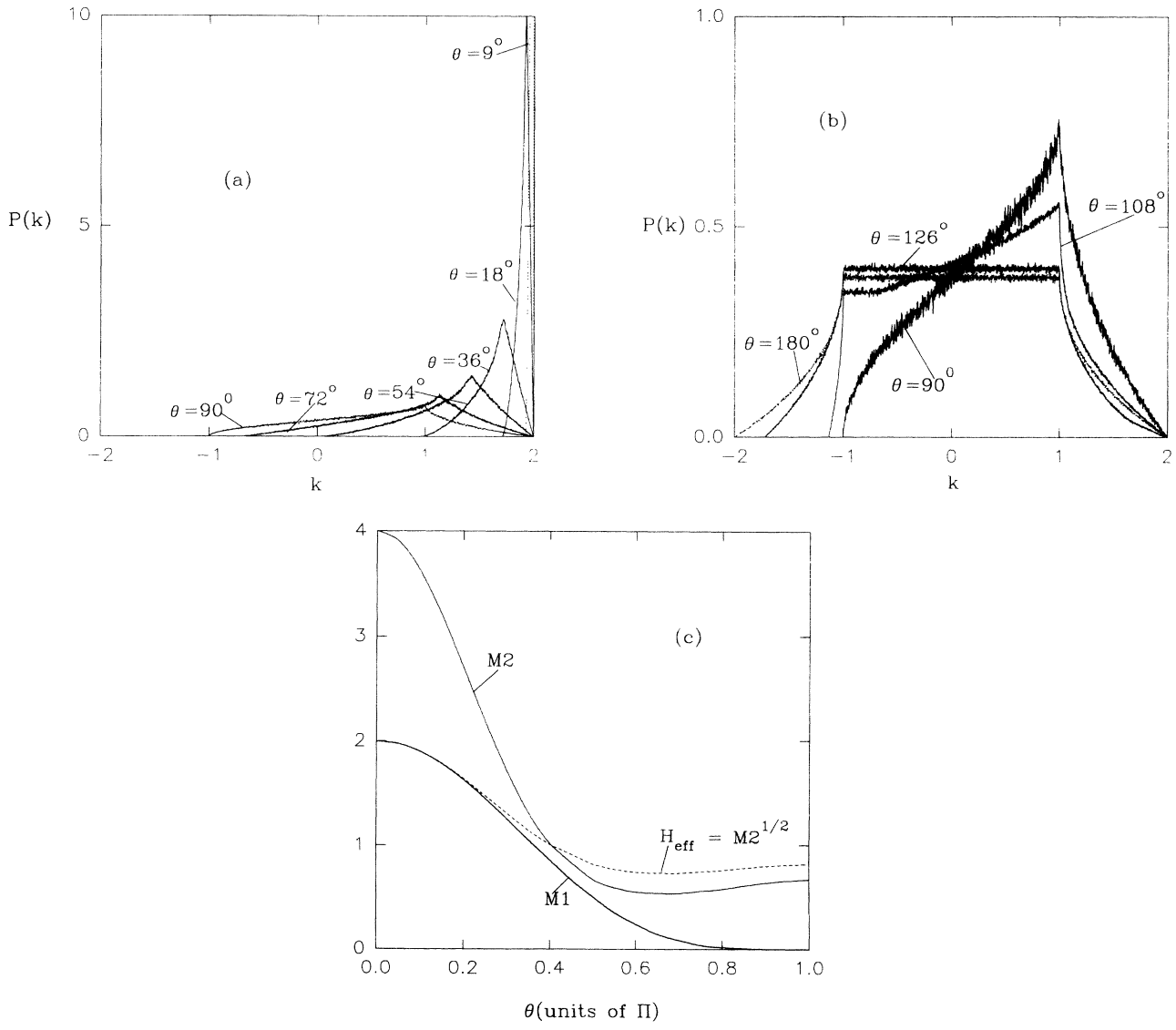

FIG. 2. The probability distribution function $P(\kappa)$ of the orientation-dependent function κ of dipole-dipole coupling is displayed in (a) and (b) for the semiangles (a) $0\le\theta_0\le\pi/2$, 10^6 points; (b) $\pi/2\le\theta_0\le\pi$, 10^7 points; (c) shows $\langle\kappa\rangle$, $\langle\kappa^2\rangle$, and $\sqrt{\kappa^2}$, denoted $M1$, $M2$, and $M2^{1/2}$, respectively.

on the cone angle through $P(\kappa)$. Subtracting the long-time value $\langle\kappa\rangle^2$ of the time correlation function and plotting it in a ln-linear plot, we can observe more easily nonexponential relaxation.

In Fig. 3(b) we display the correlation function

$$K_1^*(Dt)=\frac{K_1(Dt)-(\text{Plateau})}{K_1(0)-(\text{Plateau})} \tag{14}$$

for different semiangles θ_0. The decay of $K_1^*(\tau)$ is single exponential for $\theta_0=171°$ and 45° but multiexponentially for the intermediate angle.

C. The numerical simulation of the stochastic Liouville equation (8)

From Secs. III A and III B we have obtained the stochastic time-dependent Liouville matrix of Eqs. (9) and (10). The next step is to solve this stochastic differential equation. In the numerical calculations to be discussed, the physical parameters used are summarized in Table I. The Liouville matrix of Eq. (8) is of a special character usually denoted as stiff since two of its eigenvalues are very different from the other two. In Brownian dynamical simulations one should avoid all types of time consuming operations such as, for instance, matrix inversions. In order to solve Eq. (8), we use a symmetrized version of the Trotter formula [7] as a basis for the numerical algorithm. First we decompose the Liouville matrix into a diagonal and an off-diagonal part,

$$\frac{d}{dt}\chi(t)=-[\mathbf{L}_0+ih(t)\mathbf{L}_1]\chi(t)\ , \tag{15}$$

where the L_1 matrix has a special symmetry:

$$L_1=\begin{bmatrix}0&0&1&-1\\0&0&-1&1\\1&-1&0&0\\-1&1&0&0\end{bmatrix}, \tag{16}$$

where the stochastic time-dependent dipole-dipole coupling is manifested in the strength constant $h(t)$. The short time solution of this equation system now written with discrete time has the following form:

$$\chi_{i+1}=e^{[L_0+ih(t_i)L_1]\Delta t}\chi_i\ . \tag{17}$$

Here, $\Delta t=(t_{i+1}-t_i)$. The symmetrized version of the Trotter formula [7] is given by

$$e^{[L_0+ih(t_i)]\Delta t}=e^{L_0\Delta t/2}e^{ih(t_i)L_1\Delta t}e^{L_0\Delta t/2}+C(\Delta t^3)\ . \tag{18}$$

From Eq. (18) we obtain a finite-difference scheme of the second order provided all matrix exponentials can be exactly calculated. The calculation of the first exponential is trivial:

$$e^{L_0\Delta t/2}=\begin{bmatrix}e^{-\lambda_1\Delta t/2}&0&0&0\\0&e^{-\lambda_2\Delta t/2}&0&0\\0&0&e^{-\lambda_3\Delta t/2}&0\\0&0&0&e^{-\lambda_4\Delta t/2}\end{bmatrix}. \tag{19}$$

The calculation of the second term is less trivial but can be obtained according to the following procedure. Since $\mathbf{L}_1\mathbf{L}_1=2\mathbf{I}$, where I denotes the block diagonal matrix,

$$I=\begin{bmatrix}1&-1&0&0\\-1&1&0&0\\0&0&1&-1\\0&0&-1&1\end{bmatrix}. \tag{20}$$

We also have the following relations: $\mathbf{II}=2\mathbf{I}$ and $\mathbf{IL}_1=2\mathbf{L}_1$.

Thus, using the Taylor series, the exponential can be rewritten to

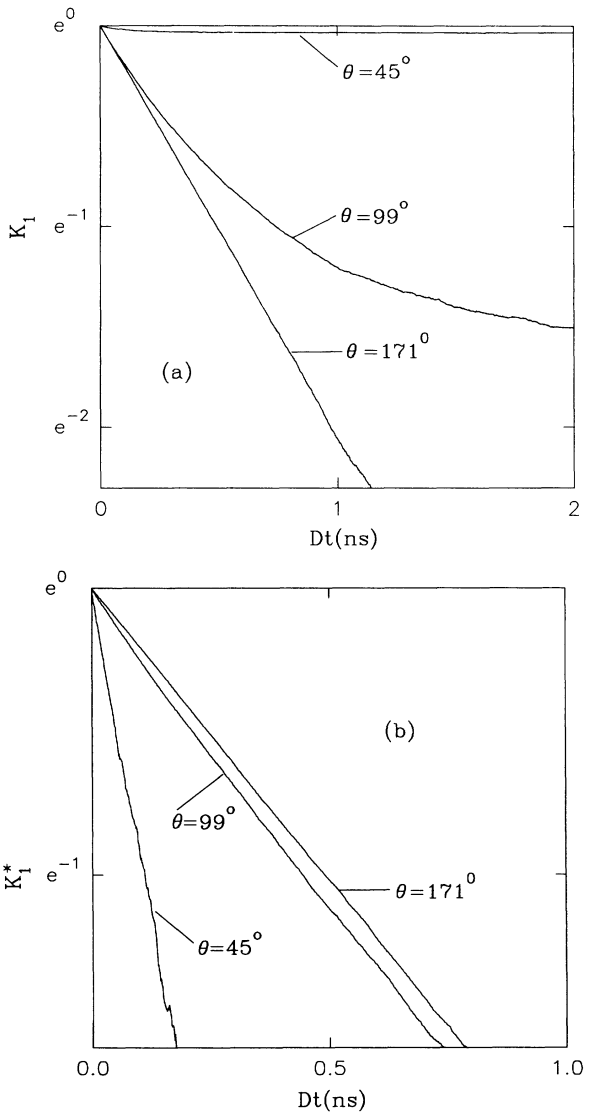

FIG. 3. The correlation functions (a) $K_1[t]=\langle\kappa(t)|\kappa(0)\rangle$ and (b) $\ln K_1^*=\ln\{K_1[t]-\langle\kappa(\Omega)\rangle\langle\kappa(\Omega)\rangle\}$ are displayed for three cone potentials defined by semiangles $\theta_0=45°$, 99°, and 171°.

TABLE I. The physical parameters used in the model calculations.

$$\frac{1}{\tau_D}=10^7\ ,\quad \frac{1}{T_2}=10^{14}\ ,\quad \frac{m_A m_D}{4\pi\varepsilon_0 r_{AD}^3}=5\times10^{11},5\times10^{14}\ ,\quad D=10^7,0.5\times10^9\ ,10^{11}$$

$$e^{ih(t_i)L_1\Delta t}=\mathbf{E}+\mathbf{I}\{\cos[2h(t_i)\Delta t]-1\}/2 +i\mathbf{L}_1\{\sin[2h(t_i)\Delta t]\}/2\ . \tag{21}$$

We then use Eq. (17) to calculate the value of the density matrix elements in the column vector $\chi(t_{i+1})$ at time $i+1$ from the value at the previous step t_i using the random value of $h(t_i)$ obtained from the BD simulation of $\kappa(\Omega)$ (Secs. III A and III B).

We close this section by summarizing the approach of solving energy transfer problems between mobile pairs of moleculers by directly simulating the stochastic Liouville equation and using explicit trajectories of the stochastic term of the Liouville superoperator, in the following points:

(a) The stochastic noise due to the reorientational motion of a chromophore is needed in the form of explicit trajectories. This stochastic fluctuation has been simulated in our particular case using a dynamic model and Brownian dynamic simulation techniques (Appendix A) but we could equally well have extracted the trajectories from other models or from molecular dynamics (MD) simulations.

(b) The dynamics of the chromophores induces a stochastic time dependence in the intermolecular transition dipole-dipole coupling. The relevance of the stochastic noise is in the modulation of the dipole-dipole coupling between the two chromphores, $\kappa(\Omega[t])$ of Eq. (5). This "noise" entering the Liouville equation of motion can be characterized by its probability distribution function $P[\kappa(\Omega[t])]$ and its correlation function $\langle\kappa(\Omega[t])\kappa(\Omega[0])\rangle$ which are needed in other theoretical approaches such as Redfiled theory or in a cumulant expansion (Sec. III B).

(c) The actual simulation of the stochastic Liouville equation has some general steps: (1). The symmetry of the dipole-dipole Liouville matrix $\mathbf{L}$ allows us to decompose it into a finite sum of Liouville matrices with the important symmetry property $\mathbf{LL}=\mathbf{I}$ and $\mathbf{LI}=k\mathbf{L}$, and (2). The Trotter formula is applied to the exponential operator $e^{\mathbf{L}t}$ and, using the Taylor series, we obtained Eq. (21), which is the main result of this paper.

IV. NUMERICAL RESULTS

In order to investigate the influence of stochastic dynamics and the configuration on the energy transfer rate, we have performed a number of numerical simulations of SLE [Eq. (9)] for different semiangles ranging from 9° to 171° and dynamics ranging from slow to fast dynamic situations. The numerical results presented in this section all refer to the same configuration schematically shown in Fig. 1. We have varied the semiangle of two equivalent cones and the diffusion constant of the reorientation (D) within the two cones, respectively. Two quantities were determined by calculating the explicit trajectories of the density matrix elements: The correlation function $\langle\chi_1(t)|\chi_1(t_0)\rangle$ describes the probability that the initially excited chromophore is still excited at a later time t, and the second correlation function of interest $\langle\chi_2(t)|\chi_1(t_0)\rangle$ describes the probability that the initially not excited chromophore is excited at a time t. Since the excitation has to be on one of the two chromophores,

$$\langle\chi_2(t)|\chi_1(t_0)\rangle=1-\langle\chi_1(t)|\chi_1(t_0)\rangle$$

as long as only energy transfer mechanism is dominating. In all calculations this condition was fulfilled.

A. $\langle\chi_1(t)|\chi_1(t_0)\rangle$ in the weak coupling regime

With the weak coupling of strong narrowing regime we refer to the regime where ordinary time-dependent perturbation theory is applicable. In this regime it is (in principle) possible to derive a generalized Förster rate master equation where the effects of molecular reorientational dynamics has been included [2]. The numerical results of this section all refer to the configuration shown schematically in Fig. 1. We have changed the semiangle of the two cones and the reorientation diffusion constant D of the two chromophores.

The ln-ln plot of Fig. 4(a) and the semilog plot of Fig. 4(b) show a family of correlation functions $\langle\chi_1(t)|\chi_1(t_0)\rangle$ obtained for a different cone semiangle θ_0 and different values of the diffusion coefficients D, all curves showing multiexpotential decay. The "plateau value" displayed in Fig. 4 is apparent because of the time axes and in fact the slow decay is due to the lifetime $1/\tau_D$. For all values of the semiangles the diffusion constants have been chosen to cover the "static," intermediate, and "fast" dynamic cases. We observe power-law behavior ($t^{-\alpha}$) in an intermediate time range. For $\theta_0\leq\pi/2$ the correlation function $\langle\chi_1(t)|\chi_1(t_0)\rangle$ is almost independent of diffusion rate D but is clearly influenced by the cone potential. For larger semiangles the influence of the diffusion constant D becomes more pronounced. Multiexpotential decay is evidently extended to longer times as the reorientation diffusion slows down. In the fast dynamic limit $D>10^{11}$, the correlation functions decay for all semiangles exactly as for an effective time-independent dipole-dipole coupling H_{eff} in the (stochastic) Liouville matrix equation (10) proportional to the root mean square value of $\kappa(H_{\text{eff}}\propto\sqrt{[\kappa^2]})$. This means that an ordinary Förster master equation is valid for sufficiently fast dynamics. It was also observed that a larger semiangle of the cone potential requires a larger value of D to guarantee that the Förster master equation is valid. This is expected since the correlation function $\langle\kappa[\Omega(0)]\kappa[\Omega(t)]\rangle$ decays faster as the cone semiangle is made smaller.

In the slow dynamical regime case, $D\leq10^7\kappa(\Omega)$ is time independent and the only source of irregularity in the system is due to initial conditions. This case is very similar

to energy transfer in a system of orientationally disordered chromphores characterized by $P(\kappa[\Omega])$ (cf. Figs. 2 and 3). Figure 5(a) demonstrates the onset of a single exponential asymptotic behavior for the correlation function $\langle\chi_1(t)|\chi_1(t_0)\rangle$. In Fig. 5(b) we have subtracted the exponential tail from all curves in order to investigate the net contributions to relaxation. The correlation functions are single exponential for high reorientational diffusion coefficients and for slow reorientational diffusion they are clearly multiexpontential. We continued the process of subtraction of the exponential tail and obtained five or six exponentials for the slow diffusion curves ($D=10^{10}$).

B. $\langle\chi_1(t)|\chi_1(t_0)\rangle$ in the strong coupled regime

For smaller intermolecular distances the dipole-dipole coupling may be in the "strong" coupling or slow-motion regime, that is, $\sqrt{\langle[H^{DD}]^2\rangle/6D} \geq 1$. The master equation approach using the Förster rate W is not valid [2].

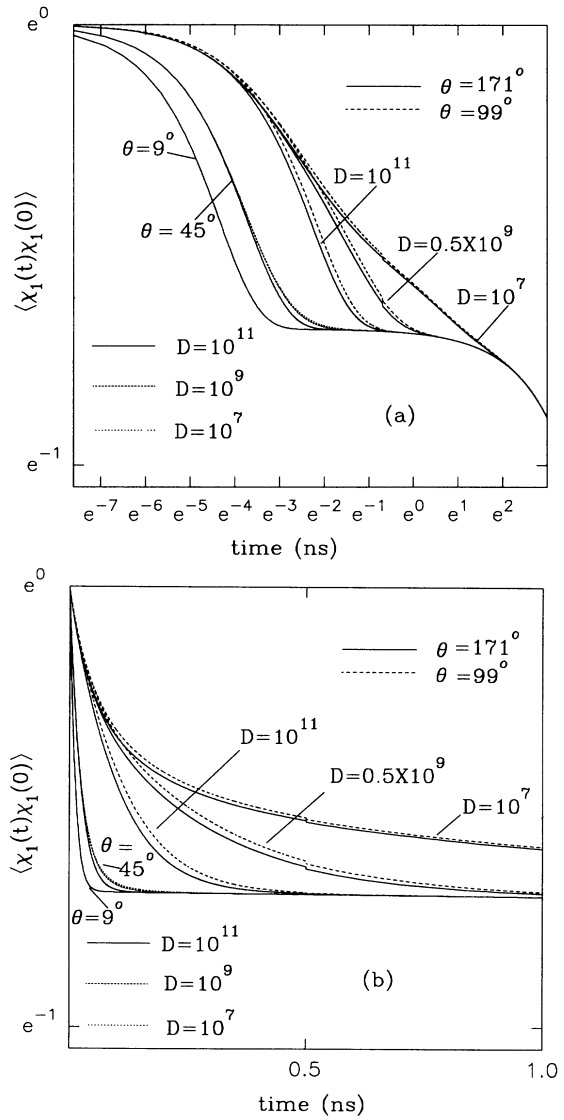

FIG. 4. The correlation function $\langle\chi_1(t)|\chi_1(t_0)\rangle$ is displayed as a function of time (a) in a ln[t]-ln plot and (b) in a semilog plot for two cone angles (99°, 171°) and three diffusion coefficients ($D=10^{10}$, 5.10^9, 10^7).

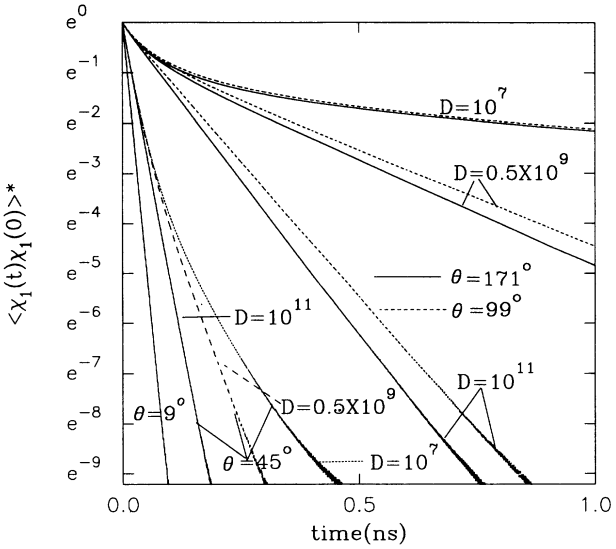

FIG. 5. The correlation function $\ln\{\langle\chi_1(t)|\chi_1(t_0)\rangle - \langle\chi_1\rangle\langle\chi_1\rangle\}$ obtained from 10^5 trajectories is displayed as a function of time for the same cone angles and diffusion coefficients as in Fig. 4.

A theoretical framework capable of treating energy transfer in the strong coupling regime is the SLE approach. However, a complication not treated explicitly in this paper is that for real applications and very fast energy transfer, the Liouville matrix must be extended to include a number of vibrational level of each chromophore and with explicit vibration relaxation rate constants. This generalization is in one sense straightforward; however, it will lead to a much larger Liouville matrix. If we still assume that the orientational dependence of the dipole-dipole coupling is independent of vibrational levels or known explicitly, we may use this approach. The principle ideas of our algorithm are still applicable since the new Liouville matrix may be decomposed into matrices with the symmetry properties required by our algorithm [Eqs. (17)–(21)].

In this section we present some results to illustrate the behavior of the correlation function $\langle\chi_1(t)|\chi_1(t_0)\rangle$ under strong coupling conditions without including vibrational relaxation processes. The main difference between the weak and the strong coupled cases is the oscillating behavior of $\langle\chi_1(t)|\chi_1(t_0)\rangle$ shown in Fig. 6 (excitation quanta jumps back and forth between chromophores before equilibrium distribution between two molecules is obtained). The relaxation is strongly dependent on cone angles but shows very weak dependence on the diffusion coefficient D.

C. The fluorescence anisotropy

The fluorescence emission anisotropy is frequently studied and is defined as

$$r(t)=\frac{I_{ZZ}(t)-I_{ZY}(t)}{I_T(t)}\ , \tag{22}$$

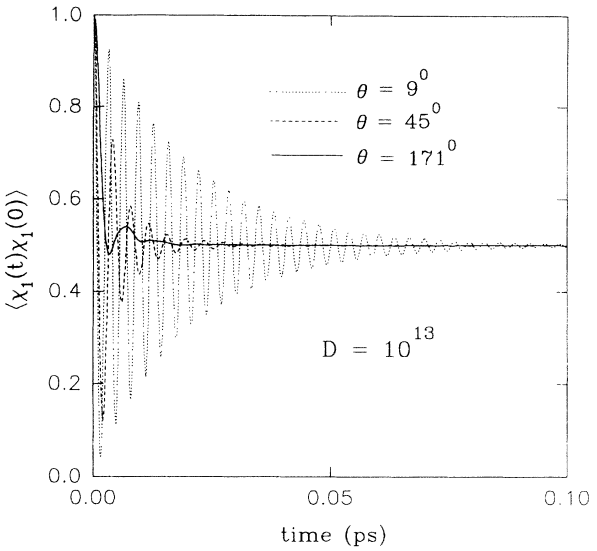

FIG. 6. The correlation function $\langle \chi_1(t)|\chi_1(t_0)\rangle$ obtained from 10^5 trajectories is shown in the strong coupled case.

where $I_T(t)$ is the total fluorescence intensity. $I_{ZZ}(t)$ and $I_{ZY}(t)$ denote the intensity of the observed light with the excitation pulse polarized along the z axis and with polarizator in the z and y directions, respectively. Following the elucidating paper by Szabo [8] the fluorescence anisotropy may be related to a correlation function (Appendix B):

$$r(t-t_0)=2\langle d^2_{00}[\beta(t)]d^2_{00}[\beta(t_0)]\rangle/I_T(t-t_0)\ . \tag{23}$$

The pair of photoactive chromphores may be embedded at different distances in the macromolecular structure. At their positions in the macromolecule the chromophores are allowed to reorient in a restricted fashion described by the "wobbling in a cone model." We introduce a frame (P) fixed in the chromophore and a second (M) fixed in the macromolecule; the wobbling in a cone dynamic is described by the Euler angles Ω_{PM}:

$$\langle d^2_{00}[\beta_{LP}(t)]d^2_{00}[\beta_{LP}(t_0)]\rangle = \sum_m e^{-t/\tau_R}\tfrac{1}{5}\langle D^2_{0m}[\Omega_{PM}(t)]D^2_{0m}[\Omega_{PM}(t_0)]\ . \tag{24}$$

The time-resolved fluorescence in their donor-donor case is given by the correlation functions

$$\langle D^2_{0m}[\Omega(t)]D^2_{0m}[\Omega(t_0)]\rangle = \sum_{j,j}\langle \chi_i(t)\chi_j(t_0)D^2_{0m}[\Omega_i(t)]D^2_{0m}[\Omega_j(t_0)]\rangle/2\ . \tag{25}$$

In Fig. 7(a) the fluorescence anisotropy $r(t)$ given by the correlation function of Eq. (25) is displayed for several different cases of wobbling dynamics and cone potentials. The overall reorientational diffusion is assumed ot be slow, $\exp(t/\tau_R)=1$. The influence of the cone potential is most evident in determining the long-time limit value of $r(t)$. In Fig. 7(b), $r(t)$ is displayed for a slow-motion case where the oscillation behavior is revealed. The long-time limit value is drastically changed for the same semiangles 90°, 72°, and 54°.

V. CONCLUSIONS

In this work we have developed an algorithm to solve the stochastic Liouville equation of motion describing energy transfer between two mobile chromophores. The approach developed requires that the molecular motions have been determined explicitly, for instance, from Brownian dynamics or molecular dynamics simulation techniques. We used the cone model and the Brownian

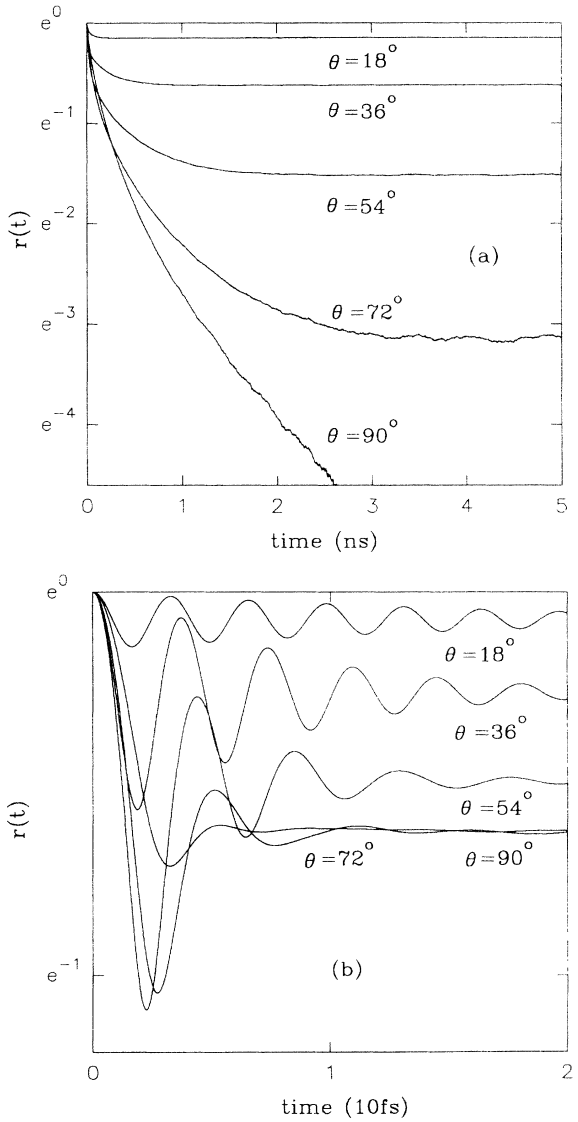

FIG. 7. The fluorescence anisotropy $r(t)$ obtained from 10^5 trajectories is displayed for different cone potentials and $D=10^9$: (a) for the weak coupled case $\{1/t_D=10^8,\ 1/T_2=10^{15},\ \mu_A\mu_D/[4\pi\varepsilon_0 r^3]=5\times10^{12}\}$, and (b) for a strong coupled case; the parameters are as in Table I.

dynamics simulation technique to determine the fluctuating dipole-dipole coupling in the stochastic Liouville matrix. The probability distribution function for the fluctuating term $\kappa(\Omega[t])$ in the dipole-dipole coupling shows non-Gaussian shape for all semiangles θ_0. This information is important if one wants to develop dynamical models using Förster's maser equation where the fluctuating Förster rate is proportional to κ^2. The algorithm was applied to solve the SLE with different wobbling dynamics, thus illustrating dynamic effects in the correlation function $\langle \chi_1(t)|\chi_1(t_0)\rangle$ and in $r(t)$, the fluorescence anisotropy. Calculations were performed in both the weak (Förster) regime and in the so-called slow-motion regime. In calculating the fluorescence anisotropy, the electronic energy transfer and the wobbling dynamics in the core are not assumed to be uncoupled.

ACKNOWLEDGMENTS

We are indebted to Dr. L.-B.-Å. Johansson for stimulating this work. This work was supported by the Swedish Natural Science Research Council and by grants from the Mat.-Nat. faculty of Umeå University.

APPENDIX A

In this appendix we review the Cartesian algorithm used in the simulation of reorientation of a chromophore in a cone potential [6]. The Langevin equations corresponding to isotropic reorientational diffusion are

$$d\theta = D\cot(\theta)dt + \sqrt{D}\, dW_\theta ,$$
$$d\phi = \sqrt{D}\frac{dW_\phi}{\sin^2\theta} , \tag{A1}$$

where W_θ and W_ϕ are standard Winer processes. These Langevin equations are not very suitable for numerical simulations due to the singularity in the $\sin^2[\theta]$. To avoid the problem of a singularity, we embedded the diffusion equation in the three-dimensional Cartesian space:

$$\frac{\partial}{\partial t}P(x,y,z,t|x_0,y_0,z_0) = \Delta_{x,y,z}P(x,y,z,t|x_0,y_0,z_0) . \tag{A2}$$

In spherical coordinates the diffusion equation of (A2) reads

$$\frac{\partial P(r,\theta,\phi,t|r_0,\theta_0,\phi_0)}{\partial t} = D\left\{\frac{1}{r_0^2}\Delta_{\theta_0\phi_0}+\Delta_{r_0}\right\}P(r,\theta,\phi,t|r_0,\theta_0,\phi_0) , \tag{A3}$$

where $P(r,\theta,\phi,t|r_0,\theta_0,\phi_0)$ is the conditional probability density and the radial part of the Laplacian operator is denoted Δ_r,

$$\Delta_r = \frac{1}{r^2}\frac{\partial}{\partial r}\left[r^2\frac{\partial}{\partial r}\right] . \tag{A4}$$

Equation (A2) is equivalent to Eq. (11), when we add the boundary condition

$$\frac{\partial}{\partial r_0}P(r,\theta,\phi,t|r_0,\theta_0,\phi_0)|_{r_0=1} = 0 , \tag{A5}$$

which must be fulfilled at every time step. This boundary condition means that the radial probability flux across the boundary should be zero. Under these conditions we may simulate the Langevin equations

$$dx = \sqrt{D}\, dW_x ,$$
$$dy = \sqrt{D}\, dW_y , \tag{A6}$$
$$dz = \sqrt{D}\, dW_z ,$$

which are extremely simple and without a singularity. The important and elaborate part of the algorithm is the realization of the two reflecting boundary conditions (A5) and (12).

The numerical version of the Langevin equations (A6) is in the form

$$x'_{i+1} = x_i + \sqrt{2Dh}\,\zeta_x ,$$
$$y'_{i+1} = y_i + \sqrt{2Dh}\,\zeta_y , \tag{A7}$$
$$z'_{i+1} = z_i + \sqrt{2Dh}\,\zeta_z ,$$

where (x_i,y_i,z_i) are the initial Cartesian coordinates of a unit vector in the cone describing the orientation of one of the chromophores at time step i and $(x'_{i+1},y'_{i+1},z'_{i+1})$ represent the position somewhere in the three-dimensional Cartesian space after time step $i+1$. h represents the time step and ζ_i are $(i=x,y,z)$ the Gaussian random numbers.

Numerical realization of additional boundary conditions (A5) [shown in Fig. 8(a)] is very simple since we can use geometrical properties of a sphere. It consists in renormalization of coordinates $\{x'_{i+1},y'_{i+1},z'_{i+1}\}$ to a new position at time $i+1$ obtained through

$$x_{i+1} = \frac{x'_{i+1}}{\sqrt{x'^2_{i+1}+y'^2_{i+1}+z'^2_{i+1}}} ,$$
$$y_{i+1} = \frac{y'_{i+1}}{\sqrt{x'^2_{i+1}+y'^2_{i+1}+z'^2_{i+1}}} , \tag{A8}$$
$$z_{i+1} = \frac{z'_{i+1}}{\sqrt{x'^2_{i+1}+y'^2_{i+1}+z'^2_{i+1}}} .$$

We know [9,10] that to satisfy the boundary conditions (12) (called "reflective"), one needs to reflect a trajectory according to their law "the angle of rejection is equal to the angle of incidence." In Fig. 8(b) a kind of complication is shown that may happen because of simulation with finite step length, namely, that the increment is so large that after the first reflection that the position vector after the renormalization $\mathbf{r}_2^i/|\mathbf{r}_2^i|$ is still outside the cone. We then proceed to find its crossing point in the cone

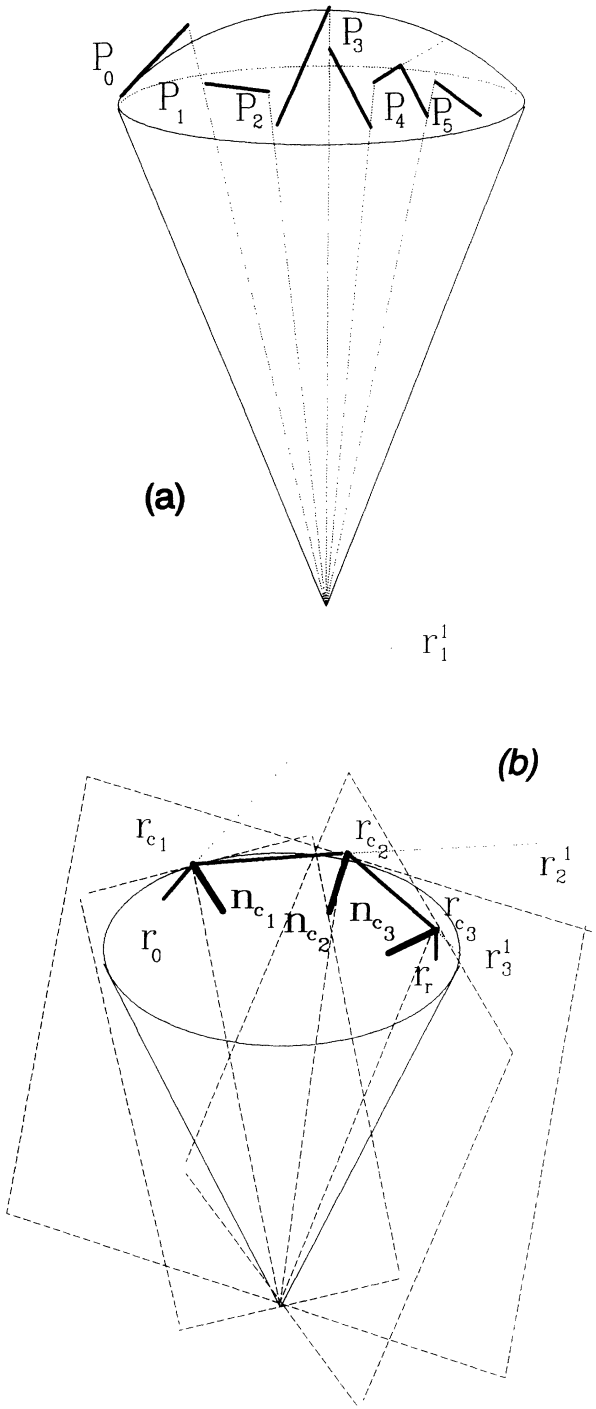

FIG. 8. (a) The renormalization procedure is schematically shown where P_i represents the position at time step 1. P_{i2} is the position after renormalization. In (b) the reflecting procedure on the spherical part of the cone is illustrated where $\mathbf{r}_{c1}$ is the first crossing point at the cone boundary and $\mathbf{n}_{c1}$ is the normal at this point. $\mathbf{r}_1^1$ is the position after the first random step, thus leaving the cone volume. $\mathbf{r}_2^1$ refers to the position after reflection of this step, however still outside the cone volume. This step crosses the cone boundary at $\mathbf{r}_{c2}$. Then we again apply the reflecting procedure in order to force the step into the cone volume having the position $\mathbf{r}_3^1$. If the normalized vector $\mathbf{r}_3^1/|\mathbf{r}_3^1|$ is on the cone, it is accepted. The planes indicated in (b) represent the tangent planes at the crossing points.

boundary n_{c2} and a new normal at this point denoted $\mathbf{n}_{c2}$ is defined. The trajectory is reflected a second time from the tangent plane to $\mathbf{r}_3^i$. If this new vector position after renormalization $\mathbf{r}_3^i/|\mathbf{r}_3^i|$ is within the cone surface, this position is accepted as the next step and

$$\mathbf{r}_3^i/|\mathbf{r}_3^i| = |\mathbf{r}^{i+1}| = |(x_{i+1}, y_{i+1}, z_{i+1})|$$

with $|\mathbf{r}^{i+1}| = 1$.

APPENDIX B

In this appendix we given the relation between the correlation function calculated and the fluorescence anisotropy $r(t)$ following the paper of Szabo [8]:

$$r(t) = \frac{I_{ZZ}(t-t_0) - I_{ZY}(t-t_0)}{I_T(t-t_0)} , \tag{B1}$$

where $I_T(t)$ is the total fluorescence intensity. $I_{ZZ}(t)$ and $I_{ZY}(t)$ denote the intensity of the observed light with excitation pulse polarized along the z axis and with polarizators in the z and y directions, respectively.

The probability $P_A(t_0)$ that the probe molecule that is excited at t_0 is proportional to the square of the projection of the transition dipole moment in the direction of the polarized excitation light used $\mu_0^{(L)}(t_0) = \cos[\beta_{LP}]$. This direction defines the z axis of the laboratory frame and in the following we use normalized transition dipole moment vectors in the spherical irreducible vector notation. The probability $P_A(t_0)$ is

$$P_A(t_0) = \tfrac{1}{3}\{1 + 2d^2_\infty[\beta_{LP}(t_0)]\} . \tag{B2}$$

The probability that the system of probe molecules emits light at a later time t with the polarization along the z and y axes of the laboratory frame, respectively, is

$$P_E(t)\tfrac{1}{3}\{1 + 2d^2_{00}[\beta(t)]\} , \tag{B3}$$

$$P_E^Y(t) = \tfrac{1}{3} - \tfrac{1}{3}d^2_{00}[\beta(t)] - \sqrt{\tfrac{1}{6}}\{d^2_{20}[\beta(t)] + d^2_{-20}[\beta(t)]\} . \tag{B4}$$

Using Eqs. (A1)–(A4), we may formulate an expression for the fluorescence anisotropy in terms of the ensemble averaged probabilities. The fluorescence anisotropy may now be written in terms of autocorrelation functions:

$$\langle P_E(t)P_A(t_0)\rangle = \tfrac{1}{9} + \tfrac{4}{9}\langle d^2_{00}[\beta(t)]d^2_{00}[\beta(t_0)\rangle , \tag{B5}$$

$$\langle P_E^Y(t)P_A(t_0)\rangle = \tfrac{1}{9} - \tfrac{2}{9}\langle d^2_{00}[\beta(t)]d^2_{00}[\beta(t_0)]\rangle . \tag{B6}$$

This gives the result of this section:

$$r(t-t_0) = 2\langle d^2_{00}[\beta(t)]d^2_{00}[\beta(t_0)]\rangle / I_T(t-t_0) . \tag{B7}$$

We introduce a principal frame (P) with its z axis defined by the direction of the transition dipole moment of the photoactive chromophore. Then in order to describe the intramolecular molecular motion of the chromophores, we introduce a molecular fixed frame with its z axis defined by the intermolecular distance vector r connecting the two chromophores attached in the macromolecule. Finally we have the laboratory fixed frame with its z axis defined by the direction of the polarizing

excitation light.

We may now relate the components of the emission dipole vector projected along the $z^{(L)}$ axis. The transformations are described by Wigner rotation matrix elements:

$$d^2_{00}[\beta_{LP}(t)] = \sum_m D^2_{0m}[\Omega_{PM}(t)] D^2_{m0}[\Omega_{ML}(t)] \ . \quad \text{(B8)}$$

Using Eq. (32), the correlation function of Eq. (31) may be determined. We assume that the overall reorientation of the macromolecule is an isotropic diffusion motion and obtain the time-resolved fluorescence anisotropy in terms of the molecular reorientational correlation functions:

$$\langle d^2_{00}[\beta_{LP}(t)] d^2_{00}[\beta_{LP}(t_0)] \rangle = \sum_m e^{-t/\tau_R} \tfrac{1}{5} \langle D^2_{0m}[\Omega_{PM}(t)] D^2_{0m}[\Omega_{PM}(t_0)] \ . \quad \text{(B9)}$$

[1] Th. Förster, Ann. Phys. (Leipzig) **2**, 55 (1948).

[2] P.-O. Westlund and H. Wennerström, J. Chem. Phys. **99**, 6583 (1993).

[3] S. Engström, M. Lindberg, and L. B.-Å. Johansson, J. Phys. Chem. **96**, 7528 (1992).

[4] V. M. Agranovich and M. D. Galanin, in *Electronic Excitation Energy Transfer in Condensed Matter* (North-Holland, Amsterdam, 1982).

[5] C. N. Banwell and H. Primas, Mol. Phys. **6**, 225 (1963).

[6] I. I. Fedchenia, P.-O. Westlund, and U. Cegrell, Mol. Simul. **11**, 373 (1993).

[7] M. Suzuki, J. Math. Phys. **26**, 601 (1985).

[8] A. Szabo, J. Chem. Phys. **81**, 150 (1984).

[9] S. Chandrasekhar, Rev. Mod. Phys. **15**, 1 (1943).

[10] I. I. Gikhman and A. V. Skhorohod, *Stochastic Differential Equations* (Springer-Verlag, Berlin, 1972).